



Intraoperative visualization and quantitative assessment of tissue perfusion by imaging photoplethysmography: comparison with ICG fluorescence angiography

VICTOR A. KASHCHENKO,^{1,2}  VALERIY V. ZAYTSEV,³ 
VYACHESLAV A. RATNIKOV,^{4,5} AND ALEXEI A. KAMSHILIN^{3,*} 

¹First Surgical Department, North-Western District Scientific and Clinical Center named after L.G. Sokolov of the Federal Medical and Biological Agency, 4 Kultury Pr., St. Petersburg 194291, Russia

²Department of Faculty Surgery, Saint Petersburg State University, 8A 21st Vasilyevskogo Ostrova Line, Saint-Petersburg 199106, Russia

³Laboratory of New Functional Materials for Photonics, Institute of Automation and Control Processes of the Far-Eastern Branch of the Russian Academy of Sciences, 5 Radio str., Vladivostok 690041, Russia

⁴Department of Radiology, North-Western District Scientific and Clinical Center named after L.G. Sokolov of the Federal Medical and Biological Agency, 4 Kultury Pr., St. Petersburg 194291, Russia

⁵Institute of Advanced Medical Technologies, Saint Petersburg State University, 8A 21st Vasilyevskogo Ostrova Line, Saint-Petersburg 199106, Russia

*alexei.kamshilin@yandex.ru

Abstract: Intraoperative monitoring of tissue perfusion is of great importance for optimizing surgery and reducing postoperative complications. To date, there is no standard procedure for assessing blood circulation in routine clinical practice. Over the past decade, indocyanine green (ICG) fluorescence angiography is most commonly used for intraoperative perfusion evaluation. Imaging photoplethysmography (iPPG) potentially enables contactless assessment of the blood supply to organs. However, no strong evidence of this potential has been provided so far. Here we report results of a comparative assessment of tissue perfusion obtained using custom-made iPPG and commercial ICG-fluorescence systems during eight different gastrointestinal surgeries. Both systems allow mapping the blood-supply distribution over organs. It was demonstrated for the first time that the quantitative assessment of blood perfusion by iPPG is in good agreement with that obtained by ICG-fluorescence imaging in all surgical cases under study. iPPG can become an objective quantitative monitoring system for tissue perfusion in the operating room due to its simplicity, low cost and no need for any agent injections.

© 2022 Optica Publishing Group under the terms of the [Optica Open Access Publishing Agreement](#)

1. Introduction

Anastomotic leakage is one of the formidable complications in many areas of surgery associated with reconstructive restoration of patency. Among various risk factors for the leakage, the blood supply to anastomosed tissues is important for both tissue healing and leakage prevention. There are various factors affecting tissue perfusion during surgery, e.g., ectomy accompanied by ligation of regional vessels, lymph node and mesentery dissection, or organ mobilization to move it to another anatomical area for anastomosis [1]. Any of them could disrupt blood circulation and become a risk factor for a leak development. The practical significance of assessing blood supply is determined by the possibility of intraoperative impact: if quantification reveals inadequate perfusion, the surgeon may change the level of resection. Various clinical signs have been suggested for intraoperative assessment of organ perfusion, including bowel serosal color, vascular pulsation, tissue bleeding, etc. However, these signs are usually subjective and may lead to misinterpretations especially in visceral obesity or damage to the serous cover of

an organ [2]. Moreover, when performing the intracorporeal anastomosis technique, in which the organ is not removed from the abdominal cavity, the capabilities of traditional methods for assessing perfusion are significantly reduced. Considering relatively high risks of postoperative complications, there is an obvious need for the development of an easy-to-use system for objective intraoperative assessment of tissue perfusion in real time.

Various optical methods such as laser Doppler flowmetry, near infrared spectroscopy, hyperspectral imaging (HSI), laser speckle contrast imaging (LSCI), sidestream darkfield microscopy (SDF), infrared thermographic imaging, optical coherence tomography (OCT), and indocyanine green fluorescence angiography (ICG-FA) have been researched as candidates for contactless intraoperative measurement of tissue perfusion [3]. Recently, four imaging modalities (LSCI, OCT, SDF, and ICG-FA) were compared on performing an intraoperative quantitative perfusion assessment during oesophagectomy. This study showed that the ICG-FA technique is the most promising for applications in real clinical conditions [4]. Application of this technique in clinical practice could help surgeons to optimize the level of resection and validate anastomosis [5–7]. However, the main disadvantage of ICG-FA evaluation is that the assessment requires a fluorescence agent ICG to be injected locally or systemically before measurements. In addition, there are problems with perfusion monitoring in the prolonged time scale: repeated ICG injections in the presence of preexisting background fluorescence make it difficult to assess tissue perfusion.

HSI is another emerging technology, which does not require administration of any fluorophore [8]. This modality combines a camera with a spectroscope and allows quantitative imaging of tissue oxygenation, which is significantly reduced in the case of vascular inflow occlusion. Recent experimental comparison of HSI and ICG-FA modalities has shown that both techniques accurately quantify and visualize real-time perfusion of the pancreas in this porcine model of pancreatic ischemia [9]. However, to the date there are only few publications describing application of this imaging modality in real clinical setting. In addition, this technique requires the use of an advanced instrument, such as imaging spectrometer.

Imaging photoplethysmography (iPPG) is an optical technique in which a conventional video camera is used to detect tiny modulations associated with blood pulsation in vessels [10,11]. This technique is contactless, extremely simple, and does not affect hemodynamic processes in living organs. It is an emerging technique that allows to sense cardiovascular signals in the outer skin layers [12]. Various research groups recently applied iPPG to monitor the vascular changes (dilatation or vasoconstriction) caused by functional tests [13–16]. These experiments suggest that the normalized amplitude of the photoplethysmography (PPG) waveform can be considered as a perfusion index. More recently, our group has demonstrated the feasibility of using iPPG to assess changes in cortical blood flow in open brain neurosurgery [17] and tissue perfusion during abdominal surgery [18]. A month later, another group from the Netherlands also demonstrated feasibility of using the iPPG technique for tissue perfusion assessment during intestinal surgery [19]. Unlike fluorescence imaging, iPPG does not need injection of any contrast agent, thus eliminating the delays associated with this preparation, and providing option of continuous monitoring over a long period of time. It should be noted that in all the cases of intraoperative perfusion assessment by the iPPG technique [17–19], no comparative analysis was carried out with alternative methods due to the lack of such technologies in most clinics. Unfortunately, to date, there is no convincing evidence that iPPG can actually be used for quantitative assessment of organ perfusion.

Verification of the applicability of the iPPG method for intraoperative assessment of tissue perfusion is a difficult task because to the date there is no instrumental technique accepted as the gold standard in the clinical setting [20]. Among the large number of non-contact optical methods, ICG-FA modality is more advanced and reliable for quantitative assessment of perfusion [4,20].

In this pilot study, we aim at comparison of a custom-made iPPG system and a commercial ICG-FA system to visualize and quantify organs perfusion during different abdominal surgeries.

The proposed imaging PPG modality allowed us to map spatial distribution of the perfusion index at several surgical steps in all eight cases studied and compare them with the relative perfusion distributions measured in parallel by the ICG-FA system. All measurements were carried out in real clinical setting. By comparing these two imaging modalities we aimed for a recommendation of the iPPG technology as possessing significant potential to aid surgeons in intraoperative perfusion assessment.

2. Patients and methods

2.1. Patients

This study was performed within the first surgical department of the North-Western District Scientific and Clinical Center of the Federal Medical and Biological Agency (Saint-Petersburg, Russia) in accordance with ethical standards presented in the 2013 Declaration of Helsinki. Approval for the study was obtained through the Ethics Committee of the North-Western District Scientific and Clinical Center, decision No 7 of May 20, 2021. All patients and/or their legal representatives provided informed consent in written form for participation in the study and for the publication of identifying information/images in an online open-access journal.

2.2. Surgical procedures

In this study, we compared performance of iPPG and ICG fluorescence imaging to quantify organs perfusion in eight different cases of abdominal surgery: gastrectomy for gastric cancer (two total cases and one distal), left hemicolectomy and sigmoid resection for left-sided colon cancer (three cases), descendrectostomy after Hartman procedure for rectosigmoid cancer, and right hemicolectomy. Medical diagnoses of the patients and types of the surgery are listed in Table 1. All these cases involved different reconstruction operations, which can be grouped according to anatomical features. Patients # 2, 5, 8 underwent gastrectomy surgery (group 1); patients # 1, 3, 4, and 7 underwent resection of the left colon (group 2), whereas patient # 6 underwent resection of the right colon (group 3).

Table 1. Patient case histories

Patient	Age (years)	Gender	Diagnosis	Surgery
1	58	f	Sigmoid colon cancer	Laparoscopically assisted sigmoid colon resection
2	62	m	Gastric cancer	Total gastrectomy
3	67	m	Rectosigmoid cancer.	Descendrectostomy after Hartman procedure and hepatic resection
4	82	f	Descending colon cancer	Laparoscopically assisted left hemicolectomy
5	71	m	Gastric cancer	Laparoscopic distal subtotal gastric resection
6	64	m	Ascending colon cancer	Laparoscopically assisted right hemicolectomy
7	72	m	Sigmoid colon cancer	Laparoscopically assisted sigmoid colon resection
8	64	m	Gastric cancer	Total gastrectomy

At the first step, the mobile part of the anastomosed complex (jejunum in the group 1, left colon in the group 2, and both ileum and transverse colon in the group 3) underwent dissection, mobilization, and then skeletonization in the area of the suggested transection. Perfusion assessment during this step can be referred to as checkout before transection. At this step, we expected that the measurement of the spatial distribution of perfusion along the organ would reveal a gradient decrease from the zone of good blood supply to the zone of no blood supply. It was important to verify that the perfusion decrease revealed by the imaging systems is not in the

resection region suggested by the surgeon, but in the removed segment of the bowel. Perfusion before transection was visualized and quantified by both systems in the group 2. In all these cases, the main decrease in perfusion was observed in the intestinal area, which is supposed to be removed. The proposed line of resection was not changed after instrumental control of the perfusion distribution.

At the second step of the reconstruction, the bowel loop (or two intestines) was prepared for anastomosis, while it was supposed to control the absence of areas with poor blood supply. We call this step the checkout before anastomosis. The aim of the perfusion visualization in the second step is to identify areas of reduced blood supply, which may indicate to the surgeon the rationality of changing the level of resection. This was done for the patients # 5, 6, 8. In these cases, no technical errors were found in the preparation of the intestine for anastomosis, the perfusion of all segments of the assessed intestine was uniform.

2.3. Experimental configuration

Intraoperative blood perfusion was monitored in parallel by the SPY Fluorescence Imaging (Stryker, Michigan, USA) and custom-made iPPG systems. Layout diagram of the study depicting the relative position of the imaging systems in relation to the patient and the general view of the operating room is shown in Fig. 1. In the panel b, to the right of the patient on the crane tripod stand, one can see the iPPG module, which is connected with a computer controlling this module, and ECG module connected both with the computer and patient. The SPY fluorescence imaging system is located to the left of the patient.

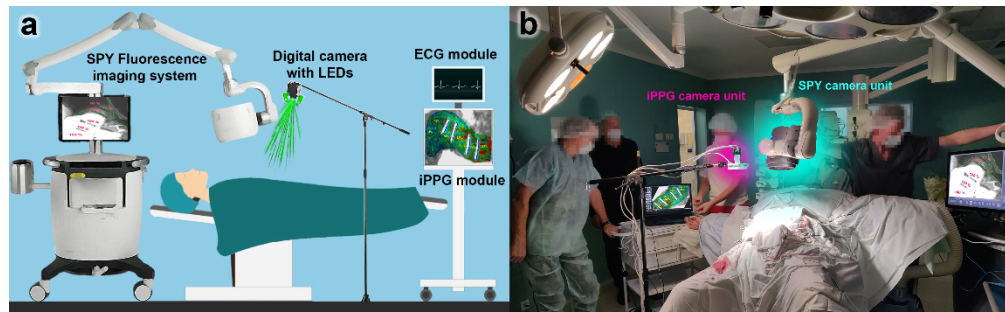


Fig. 1. Installation for intraoperative comparative monitoring of tissue perfusion. a, Layout of the experimental setup. b, Photograph of the operating room during the study. The iPPG-camera unit is highlighted in magenta while SPY-camera unit is highlighted in cyan. ECG and PPG modules provide synchronous recording of video frames and ECG.

Both systems were positioned approximately 30 - 40 cm above the region of surgery thus capturing video of the intestine from different angles (see Fig. 1(b)). Note that simultaneous monitoring of tissue perfusion by both systems was impossible due to excessive exposure of the iPPG camera to infrared radiation from the SPY system. Therefore, both systems measured perfusion sequentially with a delay between measurements of 10–30 s. Due to the difference in both viewing angles and camera lenses of the systems, spatial conformity of the regions position for perfusion assessment was manually selected by the operator (see Sect. 2.6 for details).

2.4. Imaging photoplethysmography

The iPPG system was designed and manufactured by the authors of this paper. Its key element is IDS GigE Smartek Vision GC1391MP digital camera with a Sony ICX267 photosensitive sensor possessing a maximum effective resolution of 1360×1024 pixels and the ability to acquire data in the global shutter mode. A c-mount lens KOWA LM5NCL was used with the camera, equipped

with a variable adjustable aperture $f = 1.4\text{--}16$, a minimum focusing distance of 18 cm, an angle of view of $89^\circ \times 67^\circ$ and the possibility of smooth manual focus adjustment. To provide uniform illumination of the study area, a specially designed illuminator was attached to the camera. Eight BL-HP20APGCL-5W STAR light-emitted diodes (LED) operating at the wavelength of 525 nm, with a diverging angle of 140 degrees, a luminous flux of up to 120 lumens, and a power of 5 watts were located around the lens on an aluminum plate. Linear polarizing film XP42-18 (Edmund Optics, UK) was mounted in front of the LEDs. A similar but orthogonally oriented film was installed in front of the camera lens. This polarizing filter provides the extinction ratio of 9000:1 at the wavelength of the LEDs, thereby reducing the effect of specular reflections and increasing the signal-to-noise ratio [21]. In this study we used the same iPPG system as in our recent report devoted to intraoperative visualization of tissue perfusion during abdominal surgery [18].

The camera was connected to a computer running the Windows 10 operating system via an Ethernet port. Using a crane tripod stand, the camera-illuminator module was allocated in such a way that the light incident normally on the surface of the organ under study. Installation of the iPPG module did not violate the sterility of the operating room workplace (see Fig. 1). Before recording the video, the operator set the exposure time of the camera so that the intensity of the light reflected from the organ under study was within the dynamic range of the photosensitive matrix. The images were captured using the C++ software developed in our group using the software library supplied by the camera manufacturer. The camera recorded monochrome images in uncompressed (lossless) format with a depth of 8 bits at a frequency of 39 frames per second.

Aiming for further revealing the signal associated with cardiac activity [22], we organized the recording of an electrocardiogram (ECG) simultaneously and synchronously with video frames. To this end, an electronic electrocardiograph (KAP-01 “Kardiotekhnika-EKG,” Incart Ltd., St. Petersburg, Russia) was used, which allows recording an ECG with six leads at sampling frequency of 1 kHz. In our study, we used a standard three-lead ECG recording, placing four electrodes on the patient’s extremities. To synchronize the ECG and video-data in time, the signal from the video camera was connected to the fourth ECG lead (sync pulse) via the flash-sync port of the camera. The camera was set up in such a way that at the moment when the electronic shutter was triggered, it generated a flash-sync signal, which was recorded in the fourth ECG lead. For convenience of the data monitoring during the study, the ECG signal was displayed on an additional monitor connected to a computer that controls both iPPG and ECG (see Fig. 1(a)).

2.5. Processing of iPPG data

In preparation for recording video data, the camera was positioned in such a way that the maximum area of the frame was occupied by the tissue area under study. Thereafter, the operator adjusted the camera-lens aperture and frame exposure-time so that the average pixel value in the captured image of the tissue under study was at least 150 (out of 255), and the aperture was as closed as possible to provide greater depth of field. The duration of the video recording usually ranged from 40 to 120 s, depending on the peristaltic activity of the intestine. The recorded frames with a resolution of 752×480 pixels were continuously stored in a personal computer. After the recording, these frames were processed offline by using custom software implemented on the MATLAB platform (MathWorks Inc., Natick, Massachusetts). The total time required to process the recorded data on a conventional laptop was no more than 5 minutes. Processing of the frames and synchronously recorded ECG was carried out in the following steps.

1. Digital stabilization of the tissue images was applied to minimize influence of motion artifacts by using an optical flow algorithm [23] with floating time-window. Considering multidirectional character of the motion of tissue sections caused by the peristaltic, respiratory, and cardiac activity, we divided the whole frame into 8×8 pixels segments, and applied the stabilization algorithm to each of them independently. The duration of the

floating time-window for stabilization was equal to the average cardiac cycle, determined by the positions of the R-peaks of the synchronously recorded ECG. All further calculations were carried out only with stabilized video data.

2. To reduce the processing time, the operator chose the region for the analysis in the first frame of the video, which included only the image of the organ under study. This region of analysis was limited by a closed line of arbitrary shape. It was further divided into small regions of interest (ROI) sizing 2×2 pixels, which is about $40 \times 40 \mu\text{m}$ in the tissue plane.
3. The pixel-value waveform was calculated by averaging pixel values in each ROI for every frame throughout the chosen time interval for analysis. Usually, a pixel-value waveform consists of fast-varying at the heartbeat frequency alternating component (AC) and slowly-varying component (DC) [24]. To compensate for uneven illumination, we calculated the AC/DC ratio in their absolute numerical values from the pixel-value waveform for each ROI, since both AC and DC components are directly proportional to incident light intensity [25]. After obtaining the AC/DC waveform, we linearly converted it to bipolar by subtracting the unity and inverted so that changes in the waveform are positively correlated with changes in blood pressure [16,24]. The resulting waveform is hereinafter referred to as the PPG-waveform.
4. To assess mean PPG pulse in each ROI, we split the 12-cardiac-cycles long PPG waveform into 12 parts so that each subsequent ECG R-peak was at the beginning of each time scale. By ensemble averaging the waveforms of the individual pulses of all 12 cardiac cycles, we obtained the mean PPG pulse. The difference between the maximum and minimum of the mean PPG pulse defines the amplitude of the pulsatile component (APC), a parameter that was used to map the perfusion index.
5. In this step, we completed the display of the calculated data on the screen. Parameter APC was coded in pseudo colors and its spatial distribution was overlaid with the first frame in a sequence of images lasting 12 cardiac cycles. As known, the APC parameter relates to the tone of blood supplying vessels, [16,26] and therefore, can serve as an index of perfusion.

Processing pipeline of the algorithm applied to visualize and quantify tissue perfusion by iPPG is shown in Fig. S1 in the Supplement.

2.6. Comparison of ICG-FA and iPPG systems

In the Figures below (Fig. 2 – Fig. 4 and Supplement 1 Fig. S2 – Fig. S6) we show the spatial distribution of intestinal perfusion measured by both commercial SPY Fluorescence imaging (Stryker, Michigan, USA) system and custom-made iPPG system synchronized with a digital electrocardiograph. For illustrative purposes, for each case, a color photograph of the organs under study is also shown in panels (a).

The SPY system provided a 240-second video recording showing indocyanine green fluorescence in the region under study. Data processing of the ICG fluorescent angiography was performed by the native software implemented in the SPY system. For quantitative analysis, a frame was first determined in which the mean pixel response over the whole frame reached the maximum for the entire recording. The moment corresponding to this frame was designated as the moment of maximum tissue fluorescence. Next, a small segment of the ICG recording was selected for analysis in the interval of two seconds before the moment of maximum fluorescence and two seconds after. In one of the frames of this segment, 7 to 9 regions with an area of approximately two cm^2 were selected to quantify perfusion. The fluorescence intensity in these regions was calculated by averaging the pixel values both over every region and during the selected segment of the ICG video. After determining which area has the maximum average

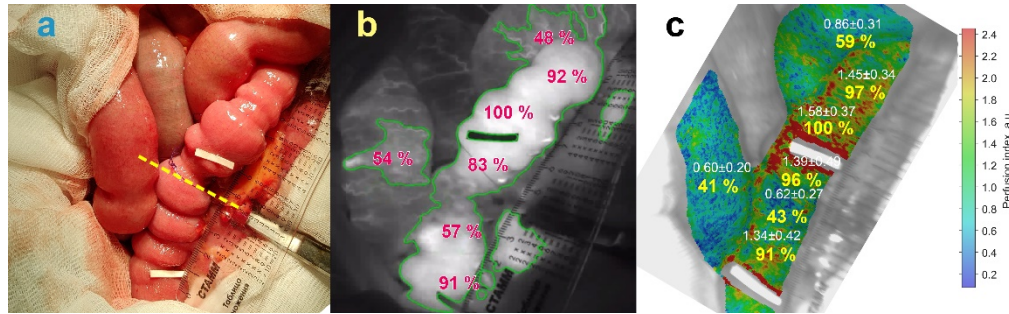


Fig. 2. Patient #2 (gastric cancer) at the first step of reconstruction before transection. **a**, Photograph of the jejunum, **b**, perfusion visualization by ICG-fluorescence imaging, and **c**, by iPPG. Dashed yellow line indicates the presuppoused resection line.

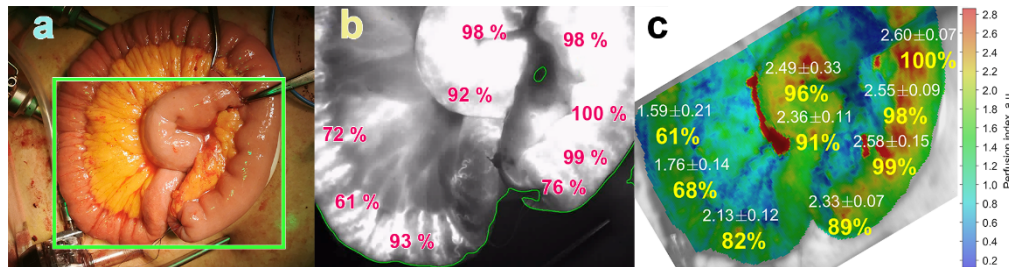


Fig. 3. Patient #5 (gastric cancer) at the second step of reconstruction. **a**, Photograph of the prepared alimentary and biliopancreatic loops, **b**, perfusion visualization by ICG-FA, and **c**, by iPPG. The green rectangle in the panel (a) indicates the location of organs in the frame for assessing perfusion.

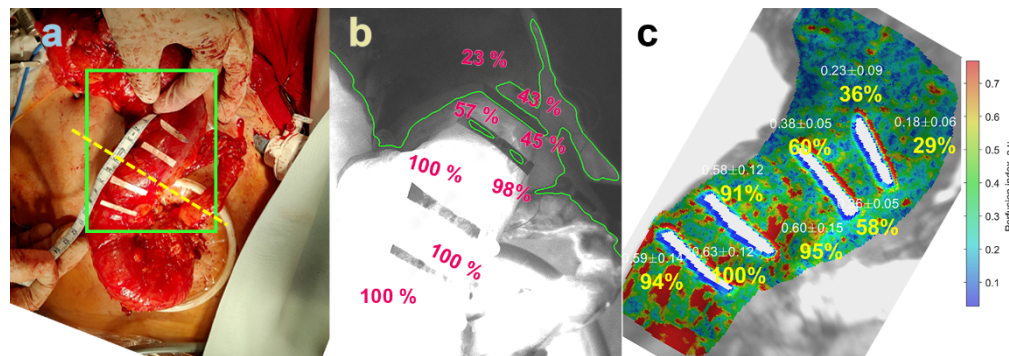


Fig. 4. Patient #1 (sigmoid colon cancer) at the first step of reconstruction (before transection). **a**, Photograph of the colon, **b**, perfusion visualization by ICG-FA, and **c**, by iPPG. Dashed yellow line indicates the presuppoused resection line.

pixel value among these selected regions, the distribution of relative perfusion (in percent) was calculated and displayed on the image of the organ under study [27]. Spatial distribution of the perfusion measured by ICG-FA is shown in panels (b) as brightness variations in the images.

As indicated in Section 2.3, perfusion was evaluated by both systems sequentially: first the measurements were carried out by the iPPG, and then by the ICG-FA system with a delay not exceeding 30 s necessary for ICG administration. ICG was injected into the peripheral vein of the patient in the form of a 5 mg bolus dissolved in 1 ml of water, immediately after the completion of iPPG measurements. It should be noted that the video recording by the iPPG system was carried out for at least five minutes in each of the 8 cases. These long-term recordings allowed us to assess for each patient how stable the iPPG system is in visualizing the distribution of perfusion in the studied organs. Since in all cases a high reproducibility of the perfusion distribution assessed by iPPG was found, we consider it legitimate to compare the distributions estimated by both systems, regardless of the sequential nature of the measurements.

The extreme values of the perfusion index observed at the borders of markers or on the dark edges of organs may be caused by the fact that the image stabilization algorithm fails when the intensity of light reflected from some parts of the image is outside the dynamic range of the camera sensor. To minimize the impact of these artifacts when comparing both systems, we averaged the perfusion parameters in regions free of artifacts, the boundaries of which were manually selected by the operator. Relative distributions of the perfusion revealed by the iPPG system were calculated in anatomically corresponding regions as in the ICG-FA images. The size of the SPY camera unit was quite large as shown in the photograph in Fig. 1(b). This does not allow us to place both camera units in such a way as to provide the same field of view (FOV). Nevertheless, averaging the responses of both systems over sufficiently large areas of the selected regions made it possible to reduce the effect of the FOV mismatch between the regions chosen by the operator during data processing. Panels (c) in the Fig. 2 to Fig. 4 and Fig. S2 to Fig. S6 in Supplement 1 show color-coded intensity maps representing spatial distribution of the intestinal perfusion index as estimated by iPPG. These maps are superimposed on the initial images of the organs under study. The areas of maximal perfusion are marked by 100% in both panels (b) and (c), whereas other numbers indicate the perfusion in other areas normalized to the respective maximal value. Relative perfusion assessed by SPY is indicated by red numbers in the panels (b). The relative perfusion (in percent) assessed by iPPG in anatomically similar areas as by the SPY is shown in yellow numbers in the panels (c). White numbers in these maps show corresponding absolute values of the index perfusion as the mean \pm standard deviation. The color scale to the right of panel (c) shows absolute value of the perfusion index as the normalized amplitude of blood pulsations [22]. The relative perfusion values assessed in the selected regions by both methods were used to estimate the correlation coefficients.

3. Results

3.1. Gastrectomy

Example of the perfusion visualization and quantification in the case of the gastrointestinal tract reconstruction by the formation of esophagojejunostomy after total gastrectomy and lymph node dissection D2 (patient #2 at the first step of operation) is shown in Fig. 2. Suggested line of the intestine transection (yellow dashed line) was marked so that the well-supplied part remains on the distal part of the intestine, which will form an alimentary loop for anastomosis with the esophagus (upper part in the Fig. 2(a)). We set two marks indicating the level of intestinal skeletonization shown by white papers in the panel (a). The distal mark is located at 1 cm from the line of resection denotes the distal border of the mesentery dissection, while the proximal mark is at 3 cm denoting the dissection border of the mesentery proximally. Between these marks is the jejunum, anatomically devoid of marginal vessels and its perfusion is possible only due to intramural collaterals.

The perfusion distribution, assessed using the ICG fluorescence (SPY) and iPPG systems is shown in panels (b) and (c), respectively. As seen in Fig. 2, both imaging techniques showed that perfusion decreased towards the intended resection line. Therefore, the high gradient between the perfusion in favorable and unfavorable zones and the high indices of tissue perfusion in the area of the intended resection line gave an additional argument to the surgeon in the correct choice of the level of bowel transection. The perfusion distributions obtained by both methods show a high correlation coefficient between them: $r = 0.89$, $P = 0.003$.

An example of perfusion visualization at the second step of reconstruction is shown in Fig. 3 for the patient #5. Here is the case of distal laparoscopic gastrectomy with D2 lymphadenectomy for cancer of the antrum. Blood supply visualization was carried out to control the perfusion of the formed biliopancreatic and alimentary loops after transection of the intestine. According to SPY, perfusion in the biliopancreatic loop in the region of the suggested anastomosis ranged from 92 to 98%, while in the alimentary loop – from 76% to 100%. IPPG revealed similar distribution of the relative perfusion (91%-96% and 89%-99% in the respective areas) and high correlation with the SPY perfusion map: $r = 0.85$, $P = 0.003$. A slight decrease in perfusion in the end zone of the alimentary loop can be explained by the marginal location of the site and invagination of the stapler line, which deforms the tissues and changes their tension.

3.2. Left colon resection

An example of gradient type perfusion observed at the first step of the reconstruction in patient #1 is shown in Fig. 4. Here we show spatial distribution of the perfusion of the left sided colon measured by ICG-FA (panel b) and iPPG (panel c) during extracorporeal stage. The yellow dashed line in the panel a indicates the level at which the dissection of the mesocolon is completed. The intestine was marked with stripes of white paper at 2.5 cm intervals. Therefore, the intestine regions below the yellow dashed line have anatomical prerequisites for blood supply (the mesocolon with the vessels is preserved), whereas above the proposed resection line, there are no such prerequisites, since the mesocolon is either cut off or the great vessels are suppressed.

As one can see, measurements of perfusion by both methods showed that a significant drop (decrease) in perfusion occurs at a distance of more than 2.5 cm from the proposed line of resection in the area of the intestine part to be removed. Both systems reveal insignificant diminishing in the perfusion at the line of the suggested resection. A high correlation was found between the distributions of perfusion measured by both methods: $r = 0.96$, $P = 0.0002$. Therefore, in this case, both methods confirmed high perfusion at the level of intestine resection and a good potential for blood supply to one of the components of the future anastomosis.

In the patient #3 presenting reconstruction after Hartman procedure for rectosigmoid cancer, the perfusion measurements were carried out prior to bowel skeletonization. This is why we did not expect significant differences in perfusion distribution. Both imaging systems showed that the perfusion of all sections of the colon is uniform and good up to the terminal sections (Fig. S3 in Supplement 1). The correlation between the SPY and iPPG perfusion distributions was also high: $r = 0.87$, $P = 0.005$.

Perfusion distribution after the sigmoid colon resection before transection can be seen in Fig. S4 in Supplement 1 for the patient #7. In this case, after sigmoid colon resection together with tumor and mesentery, the surgeon decided to change the level of resection. New level of transection was clearly defined by both imaging techniques. The correlation coefficient between the perfusion maps of ICG fluorescence and iPPG is $r = 0.89$, $P = 0.003$.

Perfusion distribution after laparoscopic resection of left segments of the colon for cancer of the descending colon at the step before transection can be seen in Supplement 1, Fig. S5 (patient # 4). After skeletonization of the colon segments that were supposed to be transected by the stapler, perfusion measurements were taken. Both imaging systems showed a correlated decrease in perfusion from the bottom of the loop to the top: $r = 0.88$, $P = 0.004$.

3.3. Right colon resection

The case of the open right hemicolectomy for cancer of the ascending colon can be seen in Supplement 1, Fig. S6, for the patient #6 at the step before anastomosis. After mobilization and resection of the right colon and 15 cm of the ileum, positioning (parallel arrangement) of the transverse colon (below) and ileum (above) was performed. Both ICG-FA and iPPG showed good perfusion of both intestines. Again, high correlation between perfusion maps obtained by both imaging techniques was observed: $r = 0.85$, $P = 0.008$.

3.4. Comparison of two methods of intraoperative perfusion assessment

The correlation coefficients of the spatial distributions of tissue perfusion estimated using ICG-FA and iPPG systems are summarized in Table 2. As one can see, the spatial distributions of the relative perfusion index revealed by both methods correlate well with each other in all the cases studied.

Table 2. Correlation of perfusion index distribution obtained by ICG-FA and iPPG systems

Patient	Number of areas	Pearson coefficient	Significance
1	8	0.96	0.0002
2	7	0.89	0.003
3	8	0.87	0.005
4	8	0.88	0.004
5	9	0.85	0.003
6	8	0.85	0.008
7	8	0.89	0.003
8	7	0.91	0.002

4. Discussion

In this study, one of the steps in the development of the safe surgery concept was presented. Obviously, maintaining sufficient blood circulation in the organs throughout the operation is important both for ensuring the fusion of the anastomosed organs and for the overall result of the intervention. However, the area of anastomosis is an Achilles' heel in the safety system, since "de novo" healing places higher demands for the perfusion parameters of the tissues to be connected by the surgeon. In this paper, we compared the performance of two non-invasive imaging modalities with tissue perfusion quantification: the established ICG fluorescence angiography and the new imaging photoplethysmography.

As key checkpoints for assessing perfusion parameters by two methods, we chose the steps during which the information obtained could influence the decision of the surgeon. The first checkpoint is the step of deciding where to transect the intestine (or intestines) involved in the anastomosis. In most cases, the transection area will be used for anastomosis, and the level of blood circulation at the transection line is an important parameter that must be strictly controlled. In no case in our series of measurements did the surgeon change the level of resection after the perfusion data were obtained. In all cases, instrumental data confirmed the safety of the surgeon's actions in relation to this step of the operation.

The second checkpoint is the assessment of intestinal perfusion immediately before anastomosis formation. Data about significant decrease in perfusion in the transection area could give reason to the surgeon to reshape the loop and change the level of resection. When assessing perfusion at this step, it was important to verify absence of its significant gradients, especially in the terminal

zone, which is used to form the anastomosis. In all studied cases, there were no significant violations of perfusion parameters, and no resection of the loop prepared for anastomosis was performed. It should be emphasized that all surgeries were performed by highly skilled surgeons with an extremely low personal risk of clinically significant failure.

Here, we demonstrate for the first time that the intraoperative tissue-perfusion distribution visualized with the custom iPPG system matches well the distributions obtained with ICG-FA. Since perfusion assessing in our iPPG system is accomplished using green light, which does not penetrate deep into the tissues due to the high concentration of red blood cells [28], the resulting match is very non-trivial. ICG-FA uses infrared light that penetrates much deeper into the tissue [6]. It is assumed that the intensity of fluorescence corresponds to the blood volume because the concentration of fluorophore is fairly uniformly distributed in the blood vessels [29]. In contrast, in photoplethysmography, after light interaction with blood vessels, its intensity turns out to be modulated in time with the heart rate [24,30]. The normalized amplitude of this modulation is considered as a marker of tissue perfusion [31,32] and used for mapping perfusion distribution in this work (see Methods). However, the question arises, how can the green light, interacting only with superficial blood vessels, assess changes in blood flow occurring in deeper, larger vessels? The answer to this question can be given within the framework of an alternative model of the PPG-waveform origin, proposed in our group in 2015 [33]. According to this model, it is the pulsating transmural pressure of the arteries that compresses/decompresses the density of superficial vessels in the tissue, thereby modulating the blood volume, which effectively absorbs green light. Due to the tissue compression by transmural pressure at the locality of the measurement, both absorption and scattering coefficients of the light are increasing that lead to corresponding changes in the reflected light intensity. Therefore, a change in the amplitude of PPG waveform may be associated with a change in arterial tone [15,16,26], which determines the blood supply. Good correlation of the perfusion maps, assessed in this study by both methods, confirms the main conclusions of the alternative model of the PPG-waveform origin.

The iPPG system enables a new technique of tissue perfusion visualization and quantization with following advantages: no needs of any substance injection, possibility of continuous perfusion monitoring, simplicity and low cost of the equipment. These features should benefit both surgeons and patients by reducing probability of postoperative complications. Applications of the technique could be easily extended to other surgical areas in which knowledge of blood circulation parameters is important: neurosurgery, vascular surgery, etc. Fusion of imaging photoplethysmography and laparoscopic technologies will allow surgeons assess organ and tissue perfusion inside the stomach and bring the surgical technique to a fundamentally new safety level. Further development of imaging photoplethysmography and deeper understanding of its physiological basis will help clarify the prognostic factors of a threatening decrease in perfusion, and the introduction of pharmacological tests will open up the possibility of drug correction of circulatory disorders.

Some limitations of the study should be mentioned. The main limitation is that it was performed in a small cohort and the data should be confirmed in a larger population. However, even in a limited number of cases we found high correlation between spatial distributions of tissue perfusion revealed by both techniques. Current limitation of the iPPG system is off-line data processing that results in a delay of about 5 minutes needed to visualize tissue perfusion. Nevertheless, we are confident that the modern computers will allow us in the nearest future to develop an iPPG system that visualizes perfusion with a delay of no more than 30 seconds.

In conclusion, a high correlation was found between the tissue perfusion maps revealed during abdominal surgery by the custom-made iPPG laboratory system and commercial ICG-FA apparatus in all eight surgical cases studied. Our study demonstrates the prospects of imaging photoplethysmography in the development of a robust clinical tool for intraoperative assessment of tissue perfusion.

Funding. Russian Science Foundation (21-15-00265).

Disclosures. The authors declare that there are no conflicts of interest related to this article.

Data availability. Data underlying the results presented in this paper are not publicly available at this time but may be obtained from the authors upon reasonable request.

Supplemental document. See [Supplement 1](#) for supporting content.

References

1. M. E. van Genderen, J. Paauwe, J. de Jonge, R. J. P. van der Valk, A. Lima, J. Bakker, and J. van Bommel, "Clinical assessment of peripheral perfusion to predict postoperative complications after major abdominal surgery early: a prospective observational study in adults," *Crit Care* **18**(3), R114 (2014).
2. A. Karliczek, N. J. Harlaar, C. J. Zeebregts, T. Wiggers, P. C. Baas, and G. M. van Dam, "Surgeons lack predictive accuracy for anastomotic leakage in gastrointestinal surgery," *Int J Colorectal Dis* **24**(5), 569–576 (2009).
3. S. M. Jansen, D. M. de Bruin, M. I. van Berge Henegouwen, S. D. Strackee, D. P. Veelo, T. G. van Leeuwen, and S. S. Gisbertz, "Optical techniques for perfusion monitoring of the gastric tube after esophagectomy: a review of technologies and thresholds," *Dis. Esophagus* **31**(6), dox161 (2018).
4. M. D. Slooter, S. M. A. Jansen, P. R. Bloemen, R. M. van den Elzen, L. S. Wilk, T. G. van Leeuwen, M. I. van Berge Henegouwen, D. M. de Bruin, and S. S. Gisbertz, "Comparison of Optical Imaging Techniques to Quantitatively Assess the Perfusion of the Gastric Conduit during Oesophagectomy," *Appl. Sci.* **10**(16), 5522 (2020).
5. R. Blanco-Colino and E. Espin-Basany, "Intraoperative use of ICG fluorescence imaging to reduce the risk of anastomotic leakage in colorectal surgery: a systematic review and meta-analysis," *Tech. Coloproctol.* **22**(1), 15–23 (2018).
6. L. van Manen, H. J. M. Handgraaf, M. Diana, J. Dijkstra, T. Ishizawa, A. L. Vahrmeijer, and J. S. D. Mieog, "A practical guide for the use of indocyanine green and methylene blue in fluorescence-guided abdominal surgery," *J Surg Oncol* **118**(2), 283–300 (2018).
7. F. Ladak, J. T. Dang, N. Switzer, V. Mocanu, C. Tian, D. Birch, S. R. Turner, and S. Karmali, "Indocyanine green for the prevention of anastomotic leaks following esophagectomy: a meta-analysis," *Surg Endosc* **33**(2), 384–394 (2019).
8. C. Chalopin, M. Maktabi, H. Köhler, F. Cervantes-Sanchez, A. Pfahl, B. Jansen-Winkel, M. Mehdorn, M. Barberio, I. Gockel, and A. Melzer, "Intraoperative Imaging for Procedures of the Gastrointestinal Tract BT - Innovative Endoscopic and Surgical Technology in the GI Tract," in *Innovative Endoscopic and Surgical Technology in the GI Tract*, S. Horgan and K.-H. Fuchs, eds. (Springer International Publishing, 2021), pp. 365–379.
9. T. Wakabayashi, M. Barberio, T. Urade, R. Pop, E. Seyller, M. Pizzicannella, P. Mascagni, A.-L. Charles, Y. Abe, B. Geny, A. Baiocchi, Y. Kitagawa, J. Marescaux, E. Felli, and M. Diana, "Intraoperative Perfusion Assessment in Enhanced Reality Using Quantitative Optical Imaging: An Experimental Study in a Pancreatic Partial Ischemia Model," *Diagnostics* **11**(1), 93 (2021).
10. T. Wu, V. Blazek, and H. J. Schmitt, "Photoplethysmography imaging: a new noninvasive and noncontact method for mapping of the dermal perfusion changes," in *Optical Techniques and Instrumentation for the Measurement of Blood Composition, Structure, and Dynamics, Proc. SPIE*, A. V. Priezzhev and P. Å. Öberg, eds. Optical Techniques and Instrumentation for the Measurement of Blood Composition, Structure, and Dynamics, Proc. SPIE (SPIE, 2000), 4163, pp. 62–70.
11. W. Verkruysse, L. O. Svaasand, and J. S. Nelson, "Remote plethysmographic imaging using ambient light," *Opt. Express* **16**(26), 21434–21445 (2008).
12. S. Zauneder, A. Trumpp, D. Wedekind, and H. Malberg, "Cardiovascular assessment by imaging photoplethysmography - a review," *Biomed. Eng. / Biomed. Tech.* **63**(5), 617–634 (2018).
13. Z. Marcinkevics, U. Rubins, J. Zaharans, A. Miscucs, E. Urtane, and L. Ozolina-Moll, "Imaging photoplethysmography for clinical assessment of cutaneous microcirculation at two different depths," *J. Biomed. Opt.* **21**(3), 035005 (2016).
14. M. A. Volynsky, N. B. Margaryants, O. V. Mamontov, and A. A. Kamshilin, "Contactless monitoring of microcirculation reaction on local temperature changes," *Appl. Sci.* **9**(22), 4947 (2019).
15. S. Rasche, R. Huhle, E. Junghans, M. G. de Abreu, Y. Ling, A. Trumpp, and S. Zauneder, "Association of remote imaging photoplethysmography and cutaneous perfusion in volunteers," *Sci. Rep.* **10**(1), 16464 (2020).
16. O. A. Lyubashina, O. V. Mamontov, M. A. Volynsky, V. V. Zaytsev, and A. A. Kamshilin, "Contactless assessment of cerebral autoregulation by photoplethysmographic imaging at green illumination," *Front. Neurosci.* **13**, 1235 (2019).
17. O. V. Mamontov, A. V. Shcherbinin, R. V. Romashko, and A. A. Kamshilin, "Intraoperative imaging of cortical blood flow by camera-based photoplethysmography at green light," *Appl. Sci.* **10**(18), 6192 (2020).
18. A. A. Kamshilin, V. V. Zaytsev, A. A. Lodygin, and V. A. Kashchenko, "Imaging photoplethysmography as an easy-to-use tool for monitoring changes in tissue blood perfusion during abdominal surgery," *Sci. Rep.* **12**(1), 1143 (2022).
19. M. Lai, S. D. van der Stel, H. C. Groen, M. van Gastel, K. F. D. Kuhlmann, T. J. M. Ruers, and B. H. W. Hendriks, "Imaging PPG for In Vivo Human Tissue Perfusion Assessment during Surgery," *J. Imaging* **8**(4), 94 (2022).
20. C. D. Lütken, M. P. Achiam, J. Osterkamp, M. B. Svendsen, and N. Nerup, "Quantification of fluorescence angiography: Toward a reliable intraoperative assessment of tissue perfusion - A narrative review," *Langenbecks Arch Surg* **406**(2), 251–259 (2021).

21. I. S. Sidorov, M. A. Volynsky, and A. A. Kamshilin, "Influence of polarization filtration on the information readout from pulsating blood vessels," *Biomed. Opt. Express* **7**(7), 2469–2474 (2016).
22. A. A. Kamshilin, T. V. Krasnikova, M. A. Volynsky, S. V. Miridonov, and O. V. Mamontov, "Alterations of blood pulsations parameters in carotid basin due to body position change," *Sci. Rep.* **8**(1), 13663 (2018).
23. J. K. Kearney, W. B. Thompson, and D. L. Boley, "Optical flow estimation: An error analysis of gradient-based methods with local optimization," *IEEE Trans. Pattern Anal. Mach. Intell.* **PAMI-9**(2), 229–244 (1987).
24. J. Allen, "Photoplethysmography and its application in clinical physiological measurement," *Physiol. Meas.* **28**(3), R1–R39 (2007).
25. H. Liu, Y. Wang, and L. Wang, "The effect of light conditions on photoplethysmographic image acquisition using a commercial camera," *IEEE J. Transl. Eng. Health Med.* **2**, 1–11 (2014).
26. M. A. Volynsky, O. V. Mamontov, A. V. Osipchuk, V. V. Zaytsev, A. Y. Sokolov, and A. A. Kamshilin, "Study of cerebrovascular reactivity to hypercapnia by imaging photoplethysmography to develop a method for intraoperative assessment of the brain functional reserve," *Biomed. Opt. Express* **13**(1), 184–196 (2022).
27. M. Sood and P. Glat, "Potential of the SPY intraoperative perfusion assessment system to reduce ischemic complications in immediate postmastectomy breast reconstruction," *Ann Surg Innov Res* **7**(1), 9 (2013).
28. R. R. Anderson and J. A. Parrish, "The optics of human skin," *J. Invest. Dermatol.* **77**(1), 13–19 (1981).
29. G. M. Son, M. S. Kwon, Y. Kim, J. Kim, S. H. Kim, and J. W. Lee, "Quantitative analysis of colon perfusion pattern using indocyanine green (ICG) angiography in laparoscopic colorectal surgery," *Surg Endosc* **33**(5), 1640–1649 (2019).
30. A. A. Kamshilin and O. V. Mamontov, "Physiological origin of camera-based PPG imaging," in *Contactless Vital Signs Monitoring*, W. Wang and X. Wang, eds. (Academic Press, 2021), pp. 27–50.
31. A. P. Lima, P. Beelen, and J. Bakker, "Use of a peripheral perfusion index derived from the pulse oximetry signal as a noninvasive indicator of perfusion," *Crit. Care Med.* **30**(6), 1210–1213 (2002).
32. A. Reisner, P. A. Shaltis, D. McCombie, and H. H. Asada, "Utility of the photoplethysmogram in circulatory monitoring," *Anesthesiology* **108**(5), 950–958 (2008).
33. A. A. Kamshilin, E. Nippolainen, I. S. Sidorov, P. V. Vasilev, N. P. Erofeev, N. P. Podolian, and R. V. Romashko, "A new look at the essence of the imaging photoplethysmography," *Sci. Rep.* **5**(1), 10494 (2015).